Title

Inositol 1,4,5-trisphosphate-mediated sarcoplasmic reticulum-mitochondrial crosstalk influences adenosine triphosphate production via mitochondrial Ca2+ uptake through the mitochondrial ryanodine receptor in cardiac myocytes.

Journal

Cardiovascular Research, 112(1)

Authors

Seidlmayer, Lea

Kuhn, Johannes

Berbner, Annette

et al.

Publication Date

2016-10-01

DOI

10.1093/cvr/cvw185

Peer reviewed

Cardiovascular Research (2016) **112**, 491–501
doi:10.1093/cvr/cvw185

Inositol 1,4,5-trisphosphate-mediated sarcoplasmic reticulum–mitochondrial crosstalk influences adenosine triphosphate production via mitochondrial Ca^{2+} uptake through the mitochondrial ryanodine receptor in cardiac myocytes

Lea K. Seidlmayer[1,2]*, Johannes Kuhn[1], Annette Berbner[1], Paula-Anahi Arias-Loza[1], Tatjana Williams[1], Mathias Kaspar[2], Martin Czolbe[1], Jennifer Q. Kwong[3], Jeffery D. Molkentin[3], Katrin Gertrud Heinze[4], Elena N. Dedkova[5], and Oliver Ritter[1,2,6]

[1]Department of Internal Medicine, Cardiology, University Hospital Würzburg, Oberdürrbacherstr. 6, 97080 Würzburg, Germany; [2]Comprehensive Heart Failure Center, University of Würzburg, Straubmühlweg 2a, 97078 Würzburg, Germany; [3]Division of Molecular Cardiovascular Biology, Cincinnati Children's Hospital Medical Center, 240 Albert Sabin Way, MLC 7020 Cincinnati, OH 45229, USA; [4]Rudolf Virchow Center for Experimental Biomedicine, University of Würzburg, Josef-Schneider-Str. 2, 97080 Würzburg, Germany; [5]Department of Pharmacology, School of Medicine, University of California Davis, 451 E. Health Sciences Drive, Genome and Biomedical Sciences Facility, Davis, CA 95616, USA; and [6]Medizinische Hochschule Brandenburg, Campus Klinikum Brandenburg/Havel, Abteilung für Kardiologie und Pneumologie, Hochstr. 29, 14770 Brandenburg an der Havel, Germany

Received 25 February 2015; revised 31 May 2016; accepted 21 June 2016; online publish-ahead-of-print 5 August 2016

Time for primary review: 35 days

Aims Elevated levels of inositol 1,4,5-trisphosphate (IP_3) in adult cardiac myocytes are typically associated with the development of cardiac hypertrophy, arrhythmias, and heart failure. IP_3 enhances intracellular Ca^{2+} release via IP_3 receptors (IP_3Rs) located at the sarcoplasmic reticulum (SR). We aimed to determine whether IP_3-induced Ca^{2+} release affects mitochondrial function and determine the underlying mechanisms.

Methods and results We compared the effects of IP_3Rs- and ryanodine receptors (RyRs)-mediated cytosolic Ca^{2+} elevation achieved by endothelin-1 (ET-1) and isoproterenol (ISO) stimulation, respectively, on mitochondrial Ca^{2+} uptake and adenosine triphosphate (ATP) generation. Both ET-1 and isoproterenol induced an increase in mitochondrial Ca^{2+} ($Ca^{2+}{}_m$) but only ET-1 led to an increase in ATP concentration. ET-1-induced effects were prevented by cell treatment with the IP_3 antagonist 2-aminoethoxydiphenyl borate and absent in myocytes from transgenic mice expressing an IP_3 chelating protein (IP_3 sponge). Furthermore, ET-1-induced mitochondrial Ca^{2+} uptake was insensitive to the mitochondrial Ca^{2+} uniporter inhibitor Ru360, however was attenuated by RyRs type 1 inhibitor dantrolene. Using real-time polymerase chain reaction, we detected the presence of all three isoforms of IP_3Rs and RyRs in murine ventricular myocytes with a dominant presence of type 2 isoform for both receptors.

Conclusions Stimulation of IP_3Rs with ET-1 induces Ca^{2+} release from the SR which is tunnelled to mitochondria via mitochondrial RyR leading to stimulation of mitochondrial ATP production.

Keywords Inositol 1,4,5-trisphosphate • IP3 sponge • Mitochondrial Ca uniporter • Mitochondrial ryanodine receptor • Dantrolene

*Corresponding author. Tel: +49 0931 201 44061; fax: +49 0931 201 44161, E-mail: seidlmayer_l@ukw.de

1. Introduction

In cardiac myocytes, large amounts of calcium (Ca^{2+}) are released from the sarcoplasmic reticulum (SR) into the cytosol with each heart beat upon activation of ryanodine receptors (RyRs). This Ca^{2+} is directed to sarcomeric structures to initiate muscle contraction. Ca^{2+} is an essential second messenger in cardiac electrical activity and is the direct activator of the myofilaments, which cause contraction. Furthermore, Ca^{2+} within the myocytes is also crucial for signalling purposes as it regulates cell metabolism, cell death, and nuclear gene transcription. The question arises how the myocyte can distinguish between global Ca^{2+} transients required for myocyte contraction and Ca^{2+} signals necessary for signalling purposes.

In addition to the RyRs, inositol 1,4,5-trisphosphate (IP_3) receptors (IP_3Rs) are also present on the SR. In contrast to RyRs, these Ca^{2+} release channels are not involved in the rhythmical Ca^{2+} release needed for excitation–contraction (EC) coupling. IP_3Rs are activated through binding of IP_3 which results in Ca^{2+} release from the SR. Although IP_3Rs are less abundant than RyRs,[1] their activation results in measurable Ca^{2+} increase during diastole and systole. It has been previously shown that IP_3-mediated Ca^{2+} release is an important regulator of nuclear gene transcription.[2,3] Furthermore, it is a critical player in the pathogenesis of cardiac diseases such as cardiac hypertrophy and heart failure.[4] Spontaneous Ca^{2+} release by IP_3Rs is one of the factors contributing to the development of arrhythmogenic events in both atrial and ventricular myocytes.[5,6]

The regulation of cellular metabolism is also Ca^{2+} dependent. By activating key enzymes of the citric acid cycle in the mitochondrial matrix, the mitochondrial matrix Ca^{2+} (together with adenine dinucleotide phosphate and inorganic phosphate) is the key regulator of adenosine triphosphate (ATP) production.[7] A number of Ca^{2+} uptake pathways have been identified in the inner mitochondrial membrane (IMM).[8–11] The mitochondrial Ca^{2+} uniporter (MCU) is the most widely studied and considered as the primary Ca^{2+} uptake pathway in mitochondria.[12–15] The properties of the MCU, however, do not allow mitochondrial Ca^{2+} uptake under physiological conditions (1–2 μM peak cytosolic Ca^{2+} concentrations during systole) because single MCU opening requires about 10–100 μM Ca^{2+} in the cytosol.[16] This is based on two important observations: (i) recent patch-clamp studies on mitoplasts have revealed a very high half-activation constant (19 mM) for the MCU,[8] and (ii) cytosolic Mg^{2+} significantly inhibits the MCU at physiological concentrations (high nanomolar range) of cytosolic Ca^{2+}.[14,17,18] Recent experimental data obtained on conditional cardiomyocyte-specific mutant mouse lacking Mcu, the pore-forming subunit of the MCU channel, do not support a significant role for the MCU in basal cardiac physiology; however cardiomyocyte-specific deletion did result in a striking inability to increase contractile function in response to the classic beta-adrenergic agonist, isoproterenol (ISO).[19,20] This raises the important questions if Ca^{2+} influx through the MCU does contribute significantly to ATP production under basal conditions, what drives mitochondrial respiratory rate and which pathway is responsible for Ca^{2+} uptake in mitochondria under normal physiological conditions?

The computational analysis[21] of Ca^{2+} dynamics in isolated cardiac mitochondria predicts two distinct models of Ca^{2+} uptake: a high affinity fast uptake pathway and a low affinity slow uptake pathway. The low affinity slow Ca^{2+} uptake pathway resembled the characteristics of the MCU; however, the high affinity fast uptake pathway was observed under physiological levels of Ca^{2+} and Mg^{2+} and could be explained only by the properties of the mitochondrial ryanodine receptor [mRyR1 (ryanodine receptor type 1 channel)] located in the IMM. The biochemical and biophysical properties of the mRyR1 are similar to those of the RyR type 1 expressed in skeletal muscles.[22] In contrast to the other RyR subtypes, the mRyR1 serves as a Ca^{2+} uptake channel. The physiological role for the mRyR1 during Ca^{2+} cycling has not been elucidated satisfactorily and remains highly controversial.

Cardiac myocytes have a highly organized structure of sarcolemma, SR, and mitochondria.[23] About 38% of the myocyte volume consists of mitochondria.[24] In ventricular myocytes, mitochondria are closely surrounded by the SR with each side neighbouring Ca^{2+} release channels on the junctional SR. In addition to this spatial relationship, dense structures connecting SR and mitochondria to each other could be seen using electron microscopy.[25] In non-excitable cells, the portion of mitochondria taking part in these microdomains was estimated to be 30% of the total number of cellular mitochondria.[26] Here, we propose that the close contact of mitochondria and the IP_3R on the SR can create Ca^{2+} fluxes that activate the mRyR1, thereby enabling Ca^{2+} uptake into the mitochondrial matrix. We tested the following hypothesis: IP_3-mediated Ca^{2+} release from the SR in close contact sites to mitochondria evokes mitochondrial Ca^{2+} uptake. This mitochondrial Ca^{2+} uptake subsequently drives ATP production. We suggest this new concept to be part of the yet unresolved question of how myocytes are able to differentiate between Ca^{2+} signals needed for contraction or signalling purposes.

2. Methods

2.1 Cell isolation

Left ventricular myocytes were isolated from 10- to 16-week-old FVB (Charles River) and IP_3 sponge mice[27] and their littermates using a Langendorff perfusion system. Prior to the procedure, mice were anaesthetized by inhalation of isofluorane. When the reflexes were absent, hearts were excised, placed into the Langendorff system and perfused with a Ca^{2+}-free washing solution, followed by an enzyme solution containing Liberase TH (Research Grade, Roche, Basel, Switzerland). Isolated myocytes were kept in Tyrode solution containing 1 mM Ca^{2+}. All protocols were in accordance with the *Guide for the Care and Use of Laboratory Animals* published by the National Institutes of Health and approved by the institutional Animal Care and Use Committee.

2.2 Confocal measurements

Laser scanning confocal microscopy (Leica SP5 and a Zeiss LSM 780) was used to follow the changes in cytosolic ($Ca^{2+}{}_i$) and mitochondrial ($Ca^{2+}{}_m$) Ca^{2+} concentration, mitochondrial membrane potential ($\Delta\Psi_m$), reactive oxygen species (ROS) generation, and mitochondrial ATP generation using specific fluorescent indicators. All fluorescence signals were recorded from individual quiescent cells incubated in Tyrode's solution containing 1 mM Ca^{2+} at room temperature. Images were recorded every 10 s. Experiments for *Figure 1G* and *H* and *Figure 3C* and *D* were performed on electrically stimulated myocytes using the same solutions and the same recording protocol as was used with the quiescent cells. Changes of fluorescence intensity are presented as background-subtracted normalized fluorescence (F/F_0) where F_0 is the initial fluorescence recorded under steady-state conditions at the beginning of each experiment. All fluorescent indicators were obtained from Molecular Probes/Life Technologies (Waltham, Massachusetts, USA) unless noted otherwise.

2.3 Ca^{2+} measurements

Ca^{2+} was measured in cytoplasm ($Ca^{2+}{}_i$) or in mitochondria ($Ca^{2+}{}_m$), using different fluorescent dyes and loading protocols. Changes in

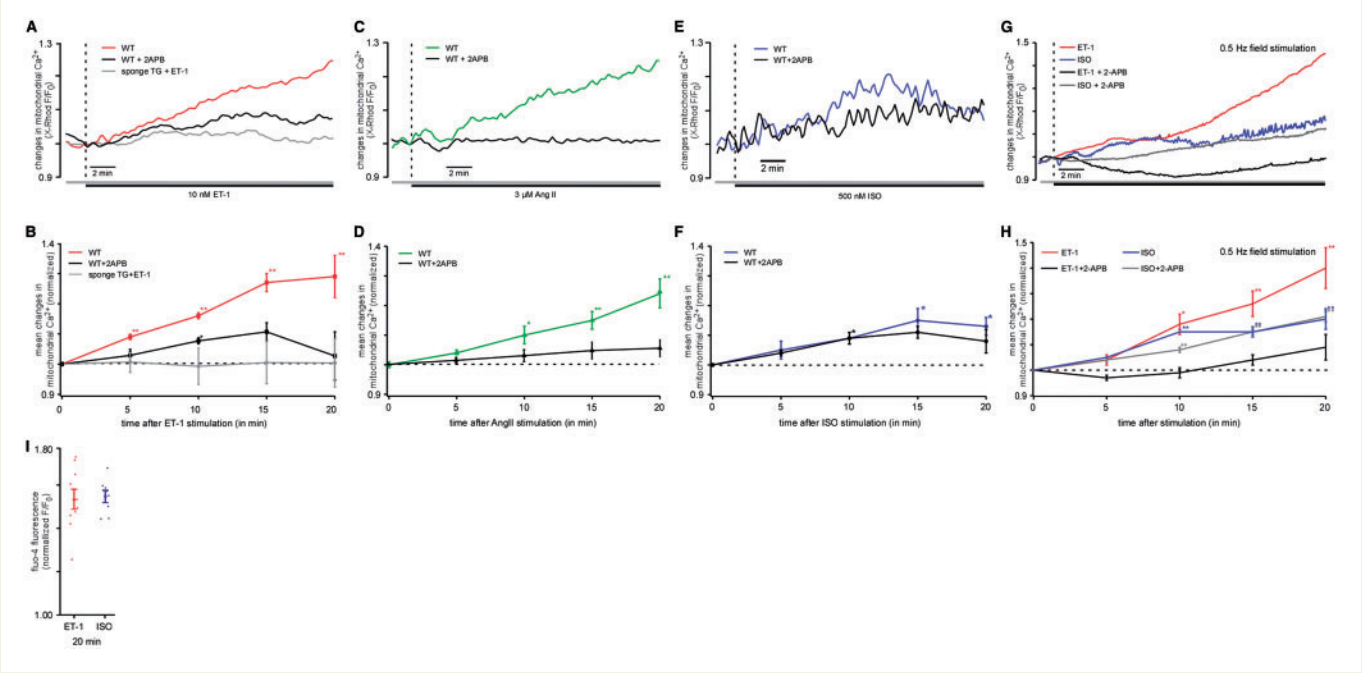

Figure 1 Mitochondrial Ca^{2+} is increased by IP_3R agonists. (*A*) Original confocal recordings obtained from WT and transgenic (sponge) myocytes stimulated with 10 nM ET-1 ± 3 μM 2-APB (red: WT, ET-1 alone; black: WT, ET-1 + 2-APB; grey: TG, ET-1 alone) for 20 min. (*B*) Mean values of resulting mitochondrial Ca^{2+} ($Ca^{2+}{}_m$) changes induced by ET-1 in WT mice in the absence ($n = 27$ from seven animals) or presence of 2-APB ($n = 19$ from four animals) and in IP_3 sponge mice [colours same as in (*A*)]. (*C*) Original confocal recordings of myocytes stimulated with 3 μM Ang II ± 3 μM 2-APB (green: Ang II; black: Ang II + 2-APB). (*D*) Mean values of resulting $Ca^{2+}{}_m$ changes induced by Ang II in the absence ($n = 10$ from three animals) or presence of 2-APB ($n = 5$ from two animals) [colours same as in (*C*)]. Both IP_3 agonists evoked a significant increase in $Ca^{2+}{}_m$, respectively. This increase could be blocked effectively by 3 μM of the IP_3 receptor blocker 2-APB and was abolished in IP_3-sponge mice. (*E*) Original confocal recordings of WT and transgenic (sponge) myocytes stimulated with 500 nM ISO ± 3μM 2-APB (blue: WT, ISO alone; black: WT, ISO + 2-APB) for 20 min. (*F*) Mean values of $Ca^{2+}{}_m$ changes induced by ISO in the absence ($n = 10$ from three animals) or presence of 2-APB ($n = 8$ from two animals) [colours same as in (*E*)]. The smaller peak and different time course indicate different underlying mechanisms. (*G*) Original confocal recordings obtained from electrically stimulated (0.5 Hz) WT myocytes stimulated with 10 nM ET-1 ± 3 μM 2-APB (red: ET-1 alone; black: ET-1 + 2-APB) or ISO ± 3 μM 2-APB (blue: ISO alone; grey: ISO + 2APB) for 20 min. (*H*) Mean values of resulting mitochondrial Ca^{2+} ($Ca^{2+}{}_m$) changes induced by ET-1 and ISO in WT mice in the absence (ET-1: $n = 6$ from three animals; ISO: $n = 7$ from two animals) or presence of 2-APB (ET-1 + 2-APB: $n = 5$ from three animals; ISO + 2-APB: $n = 11$ from two animals) [colours same as in (*G*)]. (*I*) Mean values of cytosolic Ca^{2+} levels ($Ca^{2+}{}_i$) in mouse myocytes measured with the Ca^{2+}-sensitive probe fluo-4. The myocytes were stimulated with ET-1 (red) or ISO (blue), respectively, demonstrating that both agonists induced a stable increase of $Ca^{2+}{}_i$. $^*P < 0.05$ compared with untreated control using ANOVA Dunnett's test; $^{**}P < 0.01$ compared with untreated control ANOVA Dunnett's test.

Ca^{2+} concentration are presented as relative changes in fluorescence because the calibration of non-ratiometic dyes used in our study in terms of Ca^{2+} concentration is not possible. For easier understanding of the manuscript, the relative changes in fluorescence measured by us will be termed 'Ca^{2+} concentration' throughout the manuscript. For $Ca^{2+}{}_i$ measurements, cells were loaded with 20 μM of the Ca^{2+} sensitive dye fluo-4 ($\lambda_{ex} = 488$ nm and $\lambda_{em} = 565$–605 nm) for 20 min at room temperature. $Ca^{2+}{}_m$ measurements were performed in intact cells loaded with 5 μM X-Rhod-1/AM ($\lambda_{ex} = 543$ nm and $\lambda_{em} = 552$–617 nm) for 30 min at 37 °C followed by 10 min incubation in 1 mM $CoCl_2$-containing Tyrode to quench cytosolic X-Rhod-1 fluorescence.[28,29] To rule out incomplete quenching, only myocytes with fluorescence-free nuclei and mitochondrial staining pattern were used for experiments. To block the MCU, intact myocytes were incubated in 10 μM Ru360 for 1 h at room temperature. One micromolar of Ru360 was present during the experiment. To block the mRyR1 cells were incubated in 1 μM dantrolene for 10 min, and 1 μM dantrolene was present during the experiment. To correct for photobleaching, all data obtained were normalized to an untreated control.

2.4 ROS measurements

Reactive oxygen species measurements were performed in intact cells loaded with 0.5 μM of the fluorescent probe MitoSOX Red ($\lambda_{ex} = 543$ nm and $\lambda_{em} = 555$–617 nm) which preferentially detects superoxide (O_2^-). Cells were loaded for 30 min at 37 °C. To account for MitoSOX Red fluorescence changes due to laser radiation and autofluorescence, control experiments without any treatment were performed. All data were normalized to these control data.

2.5 Mitochondrial membrane potential ($\Delta\Psi_m$) measurements

Intact myocytes were loaded using 10 nM tetramethylrhodamine methyl ester (TMRM) ($\lambda_{ex} = 543$ nm and $\lambda_{em} = 565$–605nm) for 15 min at 37 °C. To prevent TMRM wash out, all solutions used during the experiments contained 10 nM TMRM. In the end of each experiment, 5 μM carbonyl cyanide p-(tri-fluromethoxy)phenylhydrazone was added for calibration. To correct for photobleaching and autofluorescence, all data were normalized to the fluorescence levels recorded before treatment.

2.6 ATP measurements

ATP measurements were performed directly utilizing a commercially available luciferine–luciferase ATP detection assay (Invitrogen, Waltham, Massachusetts, USA, #A22066) and indirectly via the free magnesium (Mg^{2+}) concentration using the fluorescent dye mag-fluo-4 (Invitrogen) as described before.[30] This method is based on the fact that a large portion of the intracellular Mg^{2+} pool is bound to ATP and present as MgATP. As free $[Mg^{2+}]_i$ is kept constant within a rather narrow range, ATP hydrolysis leads to concomitant increase in free $[Mg^{2+}]_i$ as measured with fluorescent Mg^{2+} indicators such as mag-fluo-4.[31] Therefore, an increase in mag-fluo-4 fluorescence indicates a decrease in ATP concentration. Vice versa, a decrease in mag-fluo4-fluorescence indicates an increase in ATP concentration. For ATP measurements, myocytes were loaded with 10 μM mag-fluo-4 (λ_{ex} = 488 nm and λ_{em} = 565–605 nm) for 30 min at 37 °C. All data from these measurements are expressed as $R = 1-F/F_0$.

2.7 Quantitative real-time reverse transcription-polymerase chain reaction

Total RNA was extracted using a RNA fibrous tissue mini kit (Qiagen, Venlo, Netherlands) and cDNA synthesized from 1 μg of RNA using the iScript™ cDNA synthesis kit (Bio-Rad, Hercules, CA). Quantitative reverse transcription-polymerase chain reaction (qRT–PCR) was performed with commercial and customized TaqMan probes (Life Technologies™, Waltham, Massachusetts, USA). Target gene mRNA levels were normalized to Glyceraldehyde 3-phosphate dehydrogenase (GAPDH) which served as housekeeping gene for comparison.

2.8 IP_3-inhibited transgenic mice

As a model for functional IP_3 knockout transgenic mice were used.[23] The animals express an IP_3 chelating protein which absorbs free IP_3 in the cells (IP_3-sponge). The result is a functional IP_3 knockout model.

2.9 Statistics

All data are presented as mean ± standard error of the mean for the indicated number (n) of experiments. For comparisons of multiple groups, ANOVA was used. After a significant overall F-test, multi-group comparisons were done via Dunnett's test (including correction for multiple testing) for treatment vs. control. The real-time PCR data (*Figure 5*) were analysed using Student's t-test. Data were considered significant at $P < 0.05$.

3. Results

3.1 IP_3-mediated Ca^{2+} release mediates mitochondrial Ca^{2+} uptake

To test whether IP_3-mediated Ca^{2+} release results in mitochondrial Ca^{2+} ($Ca^{2+}{}_m$) changes, isolated murine cardiac myocytes were loaded with the Ca^{2+} sensitive fluorescent dye X-Rhod-1 under conditions which allow preferential dye loading in mitochondria (see Section 2). Therefore, observed changes in X-Rhod-1 fluorescence reflect changes in the mitochondrial Ca^{2+} concentration. To induce IP_3-mediated Ca^{2+} release, the IP_3 receptor agonist endothelin-1 (ET-1) was used to stimulate the cells. Following the addition of 10 nM ET-1 mitochondrial Ca^{2+} was significantly increased during 20 min of observation (+29 ± 3%) (*Figure 1*). To test whether this effect was specific for ET-1-mediated IP_3 release, the experiment was repeated with angiotensin II (Ang II), another IP_3R agonist. As shown in *Figure 1C* and *D*, 3 μM Ang II also significantly increased the mitochondrial Ca^{2+} concentration (+24 ± 5%). Cell treatment with 3 μM 2-aminoethoxydiphenyl borate (2-APB, IP_3R antagonist) prevented mitochondrial Ca^{2+} elevation in both ET-1- (ET-1 + 2-APB: +3 ± 8%) and Ang II-treated myocytes (Ang II + 2-APB: +6 ± 3%), demonstrating that the observed increase in mitochondrial Ca^{2+} was depending on IP_3 receptor stimulation. Furthermore, in myocytes isolated from IP_3 sponge mice (functional IP_3 knockout mice, see Section 2), the addition of ET-1 did not induce any measurable increase in mitochondrial Ca^{2+} (*Figure 1A* and *B*). These results further prove the IP_3 dependency of the observed ET-1 effects on mitochondrial Ca^{2+}. During the observation time of 20 min, a maximum in mitochondrial Ca^{2+} uptake was not reached. To exclude motion artefacts, the experiments described were performed in quiescent myocytes. As quiescent conditions in cardiac myocytes do not reflect the physiological situation, the same experimental protocol was also performed in field stimulated cells (*Figure 1G* and *H*). Here, an even more pronounced effect of ET-1 (+40 ± 8%) on mitochondrial Ca^{2+} could be seen (*Figure 1G* and *H*) which could again be blocked by 2-APB (ET-1 + 2-APB: +6 ± 5%). These data confirm that the effect observed is also relevant in contracting myocytes under physiological conditions.

3.2 Cytoplasmic Ca^{2+} increase alone is not able to mimic the effect seen after IP_3 stimulation

To test whether a cytoplasmic Ca^{2+} increase by IP_3-independent mechanisms alone is sufficient to increase mitochondrial Ca^{2+} in the same way as induced by IP_3-mediated Ca^{2+} release, the myocytes were treated with the β-adrenergic agonist ISO. We used the concentration of ISO (500 nM) which in electrically stimulated myocytes induced a stable increase in cytosolic Ca^{2+} levels as ET-1 did without evoking spontaneous activity often seen after stimulation with ISO (*Figure 1I*). This effect on cytosolic Ca^{2+} was also seen under depolarizing conditions as shown in the Supplementary material online (*Figure S1*). We determined that ISO also induced an increase in mitochondrial Ca^{2+} (*Figure 1E* and *F*). The maximum amplitude of $Ca^{2+}{}_m$ increase induced by ISO was about 50% smaller compared with the changes induced by ET-1, and this increase was not sensitive to 2-APB. The average Ca^{2+} increase following 20 min ISO stimulation was 13 ± 3% (+20 ± 4% in electrically stimulated myocytes (*Figure 1G* and *H*)) compared with +29 ± 3% $Ca^{2+}{}_m$ increase induced by ET-1. Furthermore, the kinetics of ISO-induced $Ca^{2+}{}_m$ response were clearly different from the effect on mitochondrial Ca^{2+} following ET-1 stimulation (*Figure 1F*). The maximum Ca^{2+} uptake induced by ISO was reached after 15 min then $Ca^{2+}{}_m$ slowly declined during the next 5 min of observation. When the cells where treated with ET-1, $Ca^{2+}{}_m$ continued to rise during the entire 20 min of treatment. This indicates different underlying mechanisms of the described effects on mitochondrial Ca^{2+}.

3.3 IP_3-mediated mitochondrial Ca^{2+} uptake results in mitochondrial depolarization

When mitochondria take up Ca^{2+} into their matrix in significant amounts, this Ca^{2+} uptake is accompanied by a depolarization of the mitochondrial membrane. Therefore, we measured mitochondrial membrane potential ($\Delta\Psi_m$) using the potentiometric dye TMRM. Cell treatment with 10 nM ET-1 induced $\Delta\Psi_m$ depolarization which corresponded to the increase in $Ca^{2+}{}_m$ (*Figure 2A* and *B*). Similarly to the described $Ca^{2+}{}_m$ changes, ET-1-induced $\Delta\Psi_m$ depolarization did not

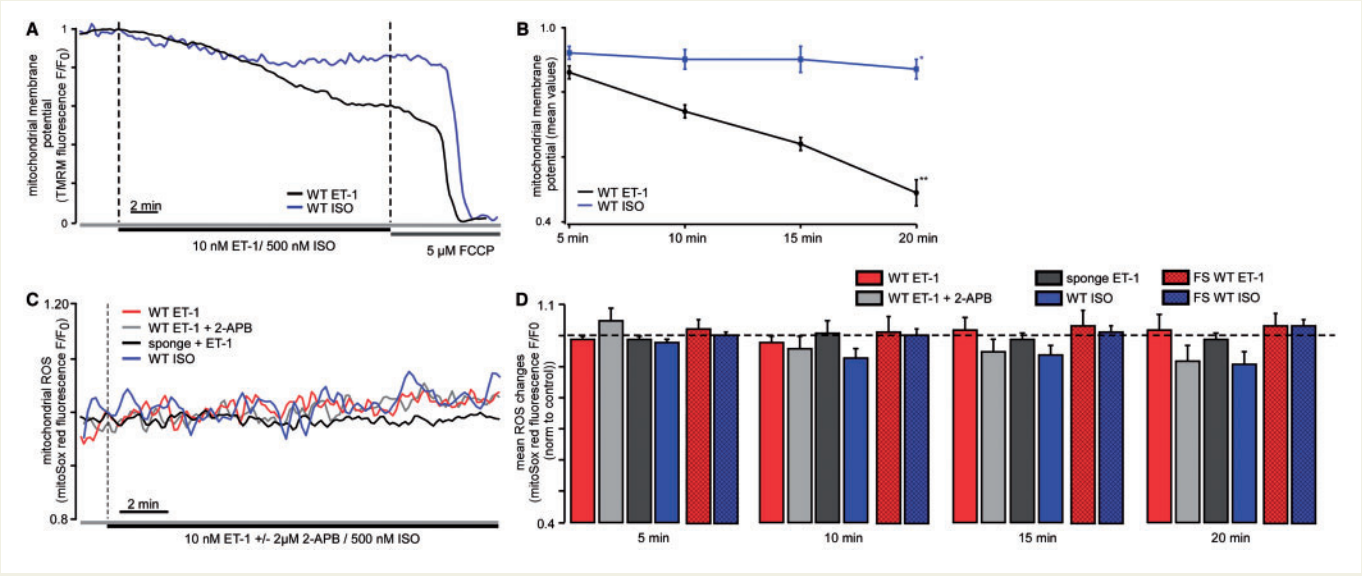

Figure 2 IP_3-mediated Ca^{2+} release results in mitochondrial membrane depolarization but does not influence ROS production. (*A*) Original confocal recordings of myocytes loaded with TMRM following ET-1 (black) and ISO (blue) stimulation. The changes in fluorescence represent the changes of the mitochondrial membrane potential ($\Delta\Psi_m$). (*B*) Mean values of $\Delta\Psi_m$ changes following ET-1 (black, $n = 9$ from two animals) and ISO (blue, $n = 9$ from four animals) over 20 min observation time. (*C*) Original confocal recordings of WT and transgenic (sponge) myocytes reflecting changes in ROS production following cellular stimulation with ET-1 ± 2-APB or ISO, respectively, in quiescent cells (red: WT + ET-1; light grey: WT + ET-1 + 2-APB; dark grey: sponge + ET-1; blue: WT + ISO) (*D*) Mean values for ROS measurements using the free radical sensor MitoSOX Red for 5, 10, 15, and 20 min. Colours same as in (*A*) (*ET-1: n = 8* from two animals, *ET-1 + 2-APB: n = 8* from one animal, sponge ET-1: $n = 6$ from two animals, ISO: $n = 9$ from two animals). Dashed bars reflect ROS generation from cells which were paced at 0.5 Hz (ET-1: $n = 7$ from two animals, ISO: $n = 14$ from three animals). Statistical differences were tested using ANOVA Dunnett's test.

reach a maximum over the observation time of 20 min (20 min ET-1: −51 ± 4%). In contrast, no significant changes in $\Delta\Psi_m$ were observed during the first 15 min of ISO (500 nM) treatment. Only after 20 min, ISO induced a significant $\Delta\Psi_m$ depolarization of −13 ± 3% (*Figure 2A and B*).

3.4 IP_3-mediated mitochondrial Ca^{2+} uptake does not stimulate mitochondrial ROS production

As the $Ca^{2+}{}_m$ concentration regulates the activity of the respiratory chain, it is likely that an increase in $Ca^{2+}{}_m$ and therefore an activation of respiration is accompanied by an increase in ROS production. Thus, we measured changes in ROS concentration using the fluorescent probe MitoSOX Red following cellular stimulation with ET-1. To correct for laser radiation-induced ROS, the fluorescence signals were normalized to an untreated control. Interestingly, no detectable ROS generation was detected following ET-1 (10 nM) stimulation in both quiescent cells (*Figures 2C and D*, open bars) and cells paced at 0.5 Hz (*Figure 2D*, dashed bars) despite the observed increase in $Ca^{2+}{}_m$ (20 min ET-1: 1 ± 5%) (*Figure 2C*). As expected, cell treatment with 3 µM 2-APB showed no significant effect on ROS levels upon ET-1 stimulation (20 min ET-1 + 2-APB: −2 ± 2%) and no increase in ROS generation was observed in cardiac myocytes from IP_3R-sponge mice (20 min ET-1: −9 ± 5%). Furthermore, in the model used by us, the cellular stimulation with 500 nM ISO was not followed by changes in ROS generation measured using the same fluorescent probe (−10 ± 4%) in both quiescent and paced cells (*Figure 2C* and *D*).

3.5 IP_3-mediated mitochondrial Ca^{2+} uptake increases mitochondrial ATP content in both quiescent and electrically stimulated cells

As the mitochondrial matrix Ca^{2+} can regulate oxidative phosphorylation at several sites, including the F_1F_0-ATPase and several dehydrogenases,[32] the impact of IP_3-mediated Ca^{2+} uptake on mitochondrial ATP production was examined. To measure the ATP concentration, two different approaches were used: (i) an indirect measurement of ATP using the magnesium (Mg^{2+}) sensitive fluorescent probe mag-fluo-4 and (ii) a commercially available luciferase assay for ATP measurements (see Section 2). The mag-fluo-4 approach is based on the fact that nearly all Mg^{2+} is bound to ATP inside the cell, and only a small fraction is free.[31] As free $[Mg^{2+}]_i$ is kept constant within a rather narrow range, any change in cellular ATP levels leads to a concomitant change in free $[Mg^{2+}]_i$. Thus, changes in $[Mg^{2+}]_i$ can be interpreted as reciprocal changes of $[ATP]_i$. In these measurements, the stimulation of myocytes with 10 nM ET-1 resulted in a significant increase (25 ± 2%) of mitochondrial ATP concentration after 20 min of stimulation (*Figure 3A* and *B*). Cell treatment with the IP_3R antagonist 2-APB prevented ET-1-induced increase in ATP (ET-1 + 2-APB: 10 ± 3% after 20 min) (*Figure 3A* and *B*). These data were confirmed in electrically stimulated myocytes in which ET-1 evoked about the same increase in ATP concentration as in quiescent myocytes (ET-1: +30 ± 5%). Similar results were obtained using a luciferase assay for ATP measurements. As shown in *Figure 3C*, IP_3R stimulation with ET-1 induced an increase in ATP content (+12 ± 14%) which was absent in myocytes from IP_3-sponge mice (−18 ± 8%).

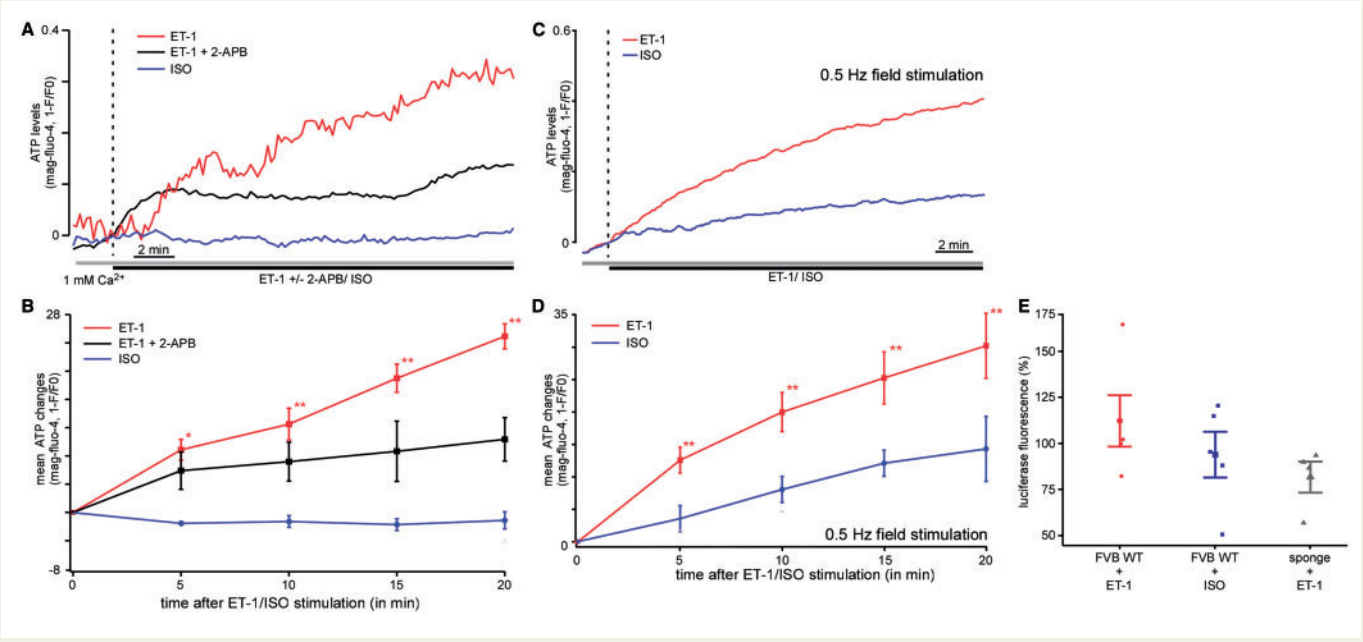

Figure 3 ATP content is increased by ET-1 but not by ISO stimulation. (*A*) Original confocal recordings of myocytes loaded with the dye mag-fluo-4. The myocytes were treated with 10 nM ET-1 (red, $n = 10$ from two animals), ET-1 plus 2-APB (black, $n = 5$ from two animals), or 500 nM ISO (blue, $n = 4$ from two animals). The changes in fluorescence represent the changes in the mitochondrial ATP concentration. (*B*) Mean values for the experiment described in (*A*). The stimulation of the cells with ET-1 induced a significant increase in mitochondrial ATP concentration after 20 min, whereas ISO had no effect. The addition of 2-APB significantly reduced the increase of mitochondrial ATP content compared with cells treated with ET-1 [colours same as in (*A*)]. (*C*) Original confocal recordings of field stimulated myocytes (0.5 Hz) loaded with the dye mag-fluo-4. The myocytes were treated with 10 nM ET-1 (red, $n = 4$ from two animals), or 500 nM ISO (blue, $n = 8$ from two animals). (*D*) Mean values for the experiment described in (*C*). (*E*) Percentage of changes of luciferase fluorescence as measurement of the cellular ATP content following ET-1 (red, $n = 5$ from five animals) and ISO (blue, $n = 5$ from four animals) in WT mouse and following ET-1 stimulation in IP_3 sponge mice (grey, $n = 4$ from four animals) measured using a luciferase assay. $^*P < 0.05$ compared with untreated control using ANOVA Dunnett's test; $^{**}P < 0.01$ compared with untreated control using ANOVA Dunnett's test.

3.6 β-adrenergic receptor activation does not result in a significant increase in mitochondrial ATP levels

As the mitochondrial Ca^{2+} increase following ET-1 stimulation markedly increased mitochondrial ATP content, we also tested the effect of β-adrenergic receptor stimulation on the mitochondrial ATP concentration using ISO. Although ISO application was associated with an increase in $Ca^{2+}{}_m$ (although less compared with ET-1 stimulation, as described above), the mitochondrial ATP content was not increased. In fact, we observed a tendency for ATP levels to decline following exposure to ISO but it was not statistically significant. Using mag-fluo-4 for indirect determination of the ATP concentration, we found no detectable changes in mitochondrial ATP concentration after 15 min exposure to 500 nM ISO in quiescent cells (−1 ± 1% at 20 min) (*Figure 3A* and *B*). These findings were confirmed using a luciferase kit for the determination of ATP concentration (−6 ± 12% ATP after 20 min ISO) (*Figure 3C*). However, in electrically stimulated myocytes (*Figure 3C* and *D*), an increase of +14 ± 3% was observed which was statistically not significant but is about half the increase observed following ET-1 indicating an increased respiratory activity in contracting myocytes compared with quiescent myocytes.

3.7 IP_3-mediated $Ca^{2+}{}_m$ uptake depends on the mitochondrial RyR1

Based on the findings described above, two different mechanisms of $Ca^{2+}{}_m$ uptake following ET-1 and ISO could be suggested. To elucidate the exact mechanism involved, we first blocked the MCU using 1 μM Ru360 (For effect of Ru360 on intact myocytes please see *Figure S2* in the Supplementary material online). Following this treatment, we stimulated the myocytes with ET-1 (*Figure 4A*) or ISO (*Figure 4B*), and measured $Ca^{2+}{}_m$ uptake using the Ca^{2+} sensitive dye X-Rhod-1 loaded into mitochondria. Interestingly, blocking the MCU did not affect ET-1-mediated $Ca^{2+}{}_m$ uptake (ET-1 alone: +29 ± 3%, ET-1 + Ru360: +31 ± 7%) but completely prevented ISO-induced $Ca^{2+}{}_m$ increase (ISO alone: +13 ± 3% and ISO + Ru360: +1 ± 2%). Therefore, the MCU clearly mediates ISO-induced $Ca^{2+}{}_m$ uptake; however, ET-1-mediated $Ca^{2+}{}_m$ uptake is independent of the MCU. The second candidate for the mediation of IP_3-induced $Ca^{2+}{}_m$ uptake was the mRyR1.[33] We, therefore, blocked the mRyR1 by cellular treatment with 1 μM of dantrolene for 10 min.[34] Following pre-incubation with dantrolene, the addition of ET-1 resulted in a significantly reduced $Ca^{2+}{}_m$ increase (ET-1 alone: +29 ± 3%, ET-1 + dantrolene: +20 ± 4% after 20 min), whereas the Ca^{2+} increase induced by ISO was not affected by dantrolene (ISO alone 13 ± 3%, ISO + dantrolene: +19 ± 3%). To test whether the described effect induced by dantrolene was mediated by an unspecific effect on the RyR type 2 (RyR2) located in the SR, myocytes were loaded with the Ca^{2+}-sensitive fluorescent probe fluo-4-AM and electrically stimulated. As demonstrated in *Figure 4C*, dantrolene had no effect on electrically induced cytosolic Ca^{2+} elevations mediated by RyR2 activation.

Next, using quantitative real-time PCR, we demonstrated the presence of all three subtypes of the RyR in wild-type (WT) murine

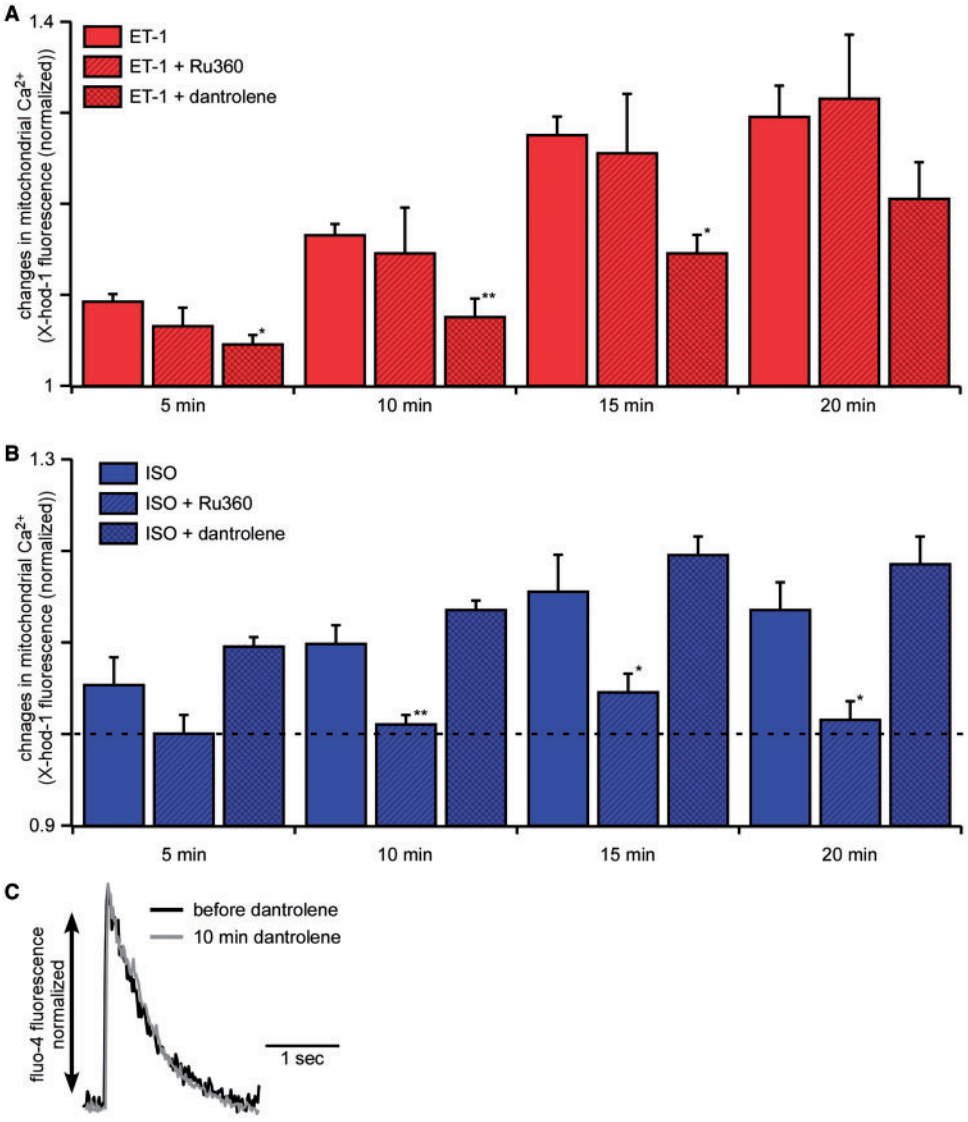

Figure 4 IP_3-mediated increase in mitochondrial Ca^{2+} is depending on the mRyR1 whereas ISO-induced mitochondrial Ca^{2+} increase is depending on the MCU. (*A*) Mean values of changes in the mitochondrial Ca^{2+} concentration following the stimulation with ET-1 (red, $n = 27$ from seven animals), ET-1 plus Ru360 (red, diagonally hatched, $n = 11$ from three animals), and ET-1 plus dantrolene (red, cross hatched, $n = 13$ from two animals). Mitochondrial Ca^{2+} uptake following the cellular stimulation with ET-1 was significantly blunted by the mitochondrial RyR blocker dantrolene. (*B*) Mean values of changes in the mitochondrial Ca^{2+} concentration following the stimulation with ISO alone (blue, $n = 10$ from three animals), ISO plus Ru360 (blue, diagonally hatched, $n = 8$ from two animals), and ISO plus dantrolene (blue, cross hatched, $n = 9$ from two animals). Mitochondrial Ca^{2+} uptake following the cellular stimulation with ISO was prevented by the MCU blocker Ru360. (*C*) Field stimulated (0.5 Hz) Ca^{2+}-transients of a murine cardiac myocyte before (black) and after 10 min of dantrolene treatment (grey). The traces are normalized and fitted to the same amplitude for the comparison of kinetics ($n = 2$ from one animal). *$P < 0.05$ compared with ET-1/ISO alone using ANOVA Dunnett's test; **$P < 0.01$ compared with ET-1/ISO alone using ANOVA Dunnett's test, respectively.

ventricular myocytes (*Figure 5A*). As expected the expression of type RyR2 was dominant in ventricular myocytes (0.3 ± 0.02). However, we also detected the presence of both RyR subtype 1 (0.008 ± 0.001) and type 3 (0.004 ± 0.0003). Furthermore, we found that the expression levels of RyR type 1 were unchanged (±0 ± 0.1%) whereas type 2 (−37 ± 7%) and type 3 (−6 ± 9%) were decreased in IP_3 sponge mice (*Figure 5B*) compared with expression levels in WT mice.

3.8 IP_3 receptor types 1 and 3 are up-regulated in cardiac myocytes from sponge mice

To elucidate which IP_3 receptor subtype is responsible for the observed $Ca^{2+}{}_m$ uptake following cellular stimulation with IP_3, we performed real-time PCR of the subtypes. Here, we could demonstrate that all three subtypes were expressed in murine cardiac myocytes with a

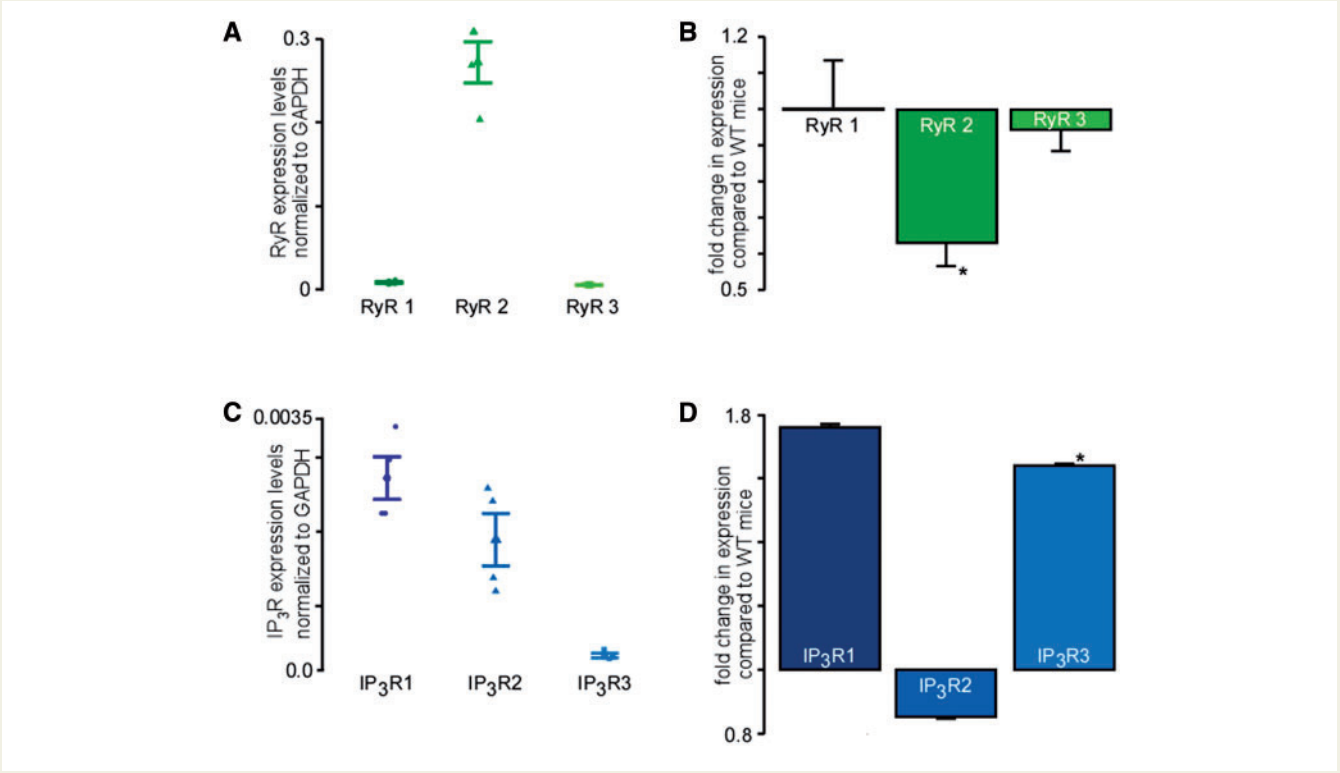

Figure 5 All three subtypes of the RyR and the IP_3R are expressed in murine cardiac myocytes. (*A*) Expression levels of three RyR subtypes normalized to GAPDH (four experiments with cells from four animals) as revealed by real-time PCR in WT murine ventricular myocytes. (*B*) Fold changes in expression levels of the three RyR subtypes in IP_3 sponge mice compared with expression levels in WT mice (four experiments with cells from four animals) (*C*) IP_3R expression levels normalized to GAPDH measured by real-time qRT–PCR (three experiments with cells from three animals). (*D*) Relative changes of IP_3R expression in cardiac myocytes of sponge mice compared with WT mice measured by real-time qRT–PCR. (three experiments with cells from three animals). *$P < 0.05$ calculated using Student's *t*-test.

predominance of IP_3R subtypes 1 and 2 (IP_3R subtype 1: 0.003 ± 0; IP_3R subtype 2: 0.002 ± 0; IP_3R subtype 3: 0.0003 ± 0) (*Figure 5C*), so that either of them could be involved in IP_3R agonist-induced increase in mitochondrial Ca^{2+} uptake and ATP generation. Interestingly, we found a significant higher expression of IP_3R subtypes 3 and 1 in IP_3 sponge mice compared with WT mice (*Figure 5D*). The expression levels of IP_3R subtype 2 were actually decreased in ventricular myocytes from IP_3 sponge mouse [IP_3R expression levels in IP_3 sponge mice compared with WT mice: IP_3R subtype 1: $+76 \pm 0.3\%$, IP_3R subtype 2: $-15 \pm 0.1\%$, IP_3R subtype 3: $+65 \pm 0.2\%$ (*Figure 5D*)]. These data imply different (patho)physiological roles for each IP_3R subtypes which need to be further investigated.

4. Discussion

The most significant finding of our studies is that agonist-induced IP_3R-mediated Ca^{2+} release is essential for the maintenance of optimal cellular bioenergetics in cardiac myocytes under normal physiological conditions in both quiescent and field-stimulated cells. In contrast, beta-adrenergic stimulation was not able to influence mitochondrial metabolism in quiescent cells, but did enhance both mitochondrial Ca^{2+} uptake and ATP levels in field-stimulated cells (*Figures 1 and 3*). However, the levels of ATP production following ISO stimulation were about 50% lower compared with the levels measured following IP_3R stimulation. Furthermore, the kinetics of mitochondrial Ca^{2+} uptake following the treatment with IP_3R and beta-receptor agonists were different as well. IP_3-mediated mitochondrial Ca^{2+} uptake induced a sustained increase in $Ca^{2+}{}_m$ levels without reaching a maximum, whereas beta-receptor stimulation was associated with a transient increase in mitochondrial Ca^{2+} concentration with a maximum reached at 15 min. Thus, we found that despite a similar increase in cytosolic $Ca^{2+}{}_i$ levels, only IP_3 agonists were able to induce a sustained increase in $Ca^{2+}{}_m$ and ATP generation, suggesting the existence of a close inter-organellar Ca^{2+} signalling. The different kinetics and effects on ATP levels imply an enduring effect of IP_3R agonists and suggest an acute effect of beta-receptor stimulation (for summary see *Figure 6*).

Our data are in agreement with the recent findings obtained on cardio-specific Mcu-deleted mice[19,20] which demonstrated that MCU matches energetic supply with cardiac workload during stress conditions. Beta-receptor stimulation with ISO induced MCU-dependent mitochondrial Ca^{2+} uptake and an acute increase in ATP production. The loss of MCU from the heart resulted in a selective inability to acutely respond to beta-adrenergic receptor stimulation or maximal forced exercise by augmenting cardiac metabolic capacity when the cardiomyocyte's work was enhanced.[20] Relative oxygen consumption rates were lower following ISO exposure in adult cardiac myocytes in Mcu-deleted cells. However, the effect was lost after chronic exposure to ISO. Importantly, MCU-deficient cardiomyocytes or deficient mice eventually catch up to controls in their contractile or metabolic performance, as

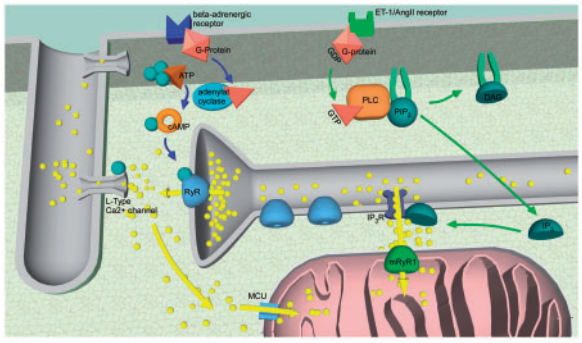

Figure 6 Summary of the proposed signalling pathways. *Shown in blue:* After ISO binds to the β-adrenergic receptor, Ca^{2+} release from the SR via the RyRs is increased (by an increased SR Ca^{2+} leak and RyR phosphorylation). The Ca^{2+} released from the SR via RyRs diffuses to mitochondria and activates the MCU. Ca^{2+} is taken up into the mitochondrial matrix. *Shown in green:* After ET-1 binds to its membrane bound receptor, the IP_3 concentration within the cell increases. Ca^{2+} from the SR is released via activated IP_3Rs. This Ca^{2+} activates the mRyR1 and is taken up in the mitochondrial matrix. Here, it activates ATP production. Blue and green arrows: second messenger actions; yellow arrows: Ca^{2+} movements; yellow balls: Ca^{2+}; green balls: phosphate.

did total Ca^{2+} load in the mitochondria. Altogether, these data suggest the existence of an alternative mechanism required to maintain mitochondrial respiration and ATP generation under basal physiological conditions, and the IP_3–mRyR1 pathway could be a candidate for this role.

Furthermore, under basal conditions total cardiomyocyte cytosolic Ca^{2+}-transient kinetics and amplitude were unaltered in myocytes from cardio-specific Mcu-deleted mice ($Mcu^{fl/fl\text{-}MCM}$) compared to $Mcu^{fl/fl}$ controls. On top, neither Ca^{2+} spark frequency and characteristics (amplitude, duration) or SR Ca^{2+} load was different in $Mcu^{fl/fl\text{-}MCM}$ myocytes compared with controls. Taken together, these results demonstrate that MCU-mediated mitochondrial Ca^{2+} import neither contributes to overall cardiac Ca^{2+} cycling in the heart nor is required to support normal cardiac function and adaptation with aging.[20] Also, mitochondrial respiration and ATP generation under basal conditions were not affected by Mcu deletion; however, when mitochondrial respiration was measured in the presence of high Ca^{2+} (100 μM external Ca^{2+}, i.e. imitating conditions of the mitochondrial Ca^{2+} overload during acute stress) both Mcu deletion and inhibition of the MCU with Ru360 led to the inhibition of the mitochondrial respiration and ATP generation.

In our study, ISO also activated acute mitochondrial Ca^{2+} uptake via the MCU. However, in contrast to ET-1 stimulation, ISO stimulation was not followed by a significant increase in ATP levels which indicates that, despite an increase in ATP generation to match the increased cellular energetic needs, the rate of ATP hydrolysis induced by ISO was higher than ATP generation. This implies that despite the activation of respiratory chain activity described by Kwong *et al.*,[20] the total amount of ATP cannot be maintained. This is in line with the finding of O-Uchi *et al.*[35] who also did not find an increase in ATP concentration following MCU stimulation but demonstrated an increase in mitochondrial ATP concentration in mRyR1 overexpressing cardiac H9c2 myoblasts. Additionally, a recent study from Andrew Marks' lab demonstrated that diastolic SR Ca^{2+} leak via type 2 RyRs causes mitochondrial Ca^{2+} overload and dysfunction in a murine model of post-myocardial infarction heart failure.[36] The exact mechanism how the enhanced type 2 RyR leak results in mitochondrial Ca^{2+} overload was not determined but the enhanced SR Ca^{2+} leak was associated with a decline in mitochondrial ATP levels. Importantly, the Marks' study found that type 2 IP_3Rs did not contribute to mitochondrial dysfunction. The study of Kwong *et al.*[20] confirmed that MCU mediates acute mitochondrial Ca^{2+} overload *in vivo* following cardiac ischaemia-reperfusion. Under these conditions, mitochondrial Ca^{2+} uptake, mitochondrial permeability transition pore (mPTP) opening, and cell death were decreased by Mcu deletion resulting in 50% decrease in infarct size.

The different actions following the activation of P_3R and beta-adrenergic receptors imply the activation of different molecular pathways. In our study, the second major finding was that Ca^{2+} released via P_3R from the SR was taken up into mitochondria by the RyR type 1 (mRyR1) whereas Ca^{2+} released via beta-adrenergic stimulation was taken up into mitochondria via the MCU (*Figure 4; see Figure 6 for summary*). So far, the physiological function of the mRyR1 has not been elucidated and after its detection in the mitochondrial inner membrane, the role of the mRyR1 in $Ca^{2+}{}_m$ cycling remains unclear.[22,33] The existence of all three types of the RyRs in cardiac myocytes was demonstrated previously with RyR type 1 located on the IMM.[22] Now, our data suggest a crucial role of the mRyR1 together with the IP_3R in the adaption of the mitochondrial metabolism to the cell's energetics needs. This finding is based on experiments in which the presence of dantrolene, a known blocker of the RyR type 1 and the mRyR1 which are structurally related, suppressed $Ca^{2+}{}_m$ uptake following ET-1. As shown by us (*Figure 4C*) and others,[37] dantrolene had no effect on cardiac EC-coupling in young mice. This excludes significant contribution of RyR2 blocking by dantrolene as a confounder to our results.

Our data demonstrate that the MCU is not involved in IP_3-mediated $Ca^{2+}{}_m$ uptake; however, it mediates $Ca^{2+}{}_m$ uptake triggered by ISO. This is in line with other publications demonstrating that Ca^{2+} is taken up into the mitochondrial matrix via the MCU during the EC-coupling cycle.[38,39] Hajnoczky and his group[40] demonstrated that Ca^{2+} released from the endoplasmic reticulum via IP_3R increased the $Ca^{2+}{}_m$ concentration in permeabilized hepatocytes which is in accordance to our findings in intact cardiac myocytes. The activation of mRyR1 by IP_3-mediated signals and not by global cytosolic Ca^{2+} indicates that cellular bioenergetics in cardiac myocytes are precisely controlled by local targeted Ca^{2+} transfer from the SR. It was shown before that mitochondria and the SR are linked physically.[25] These structures may shield IP_3R release sites from the cytosol. Furthermore, the mRyR1 is regulated by Ca^{2+} in a similar fashion as the RyR1 from skeletal muscles.[3,41] Both mRyR1 and the RyR1 are activated by low Ca^{2+} concentrations (1–10 μM) and inactivated by high Ca^{2+} concentrations (1–10 mM) which would prevent mitochondria from Ca^{2+} overload and enable localized Ca^{2+} signalling.[41] The mRyR1 shows a bell-shaped Ca^{2+}-dependent activation in a physiological range of $Ca^{2+}{}_i$ from 0.1 to ~10–30 μM Ca^{2+}. This unique property makes mRyR1 an ideal candidate for sequestering Ca^{2+} quickly and transiently under physiological $Ca^{2+}{}_i$ oscillations observed during each heartbeat. The molecular identity of RyR1 in cardiac mitochondria was carefully analysed and confirmed using not only native cardiomyocytes but also those obtained from RyR1 knockout mouse hearts.[22] Interestingly, in RyR1 knockout mouse heart mitochondria, the respiratory control index was very low (≅1). An increase in $Ca^{2+}{}_i$ did not stimulate O_2 consumption, suggesting that mRyR1 is required for both the basal metabolic state and Ca^{2+}-dependent acceleration of the TCA cycle in cardiomyocytes[22] even though its expression level was much lower

compared with the RyR2, which is the main RyR isoform in the cardiac SR.[42] Furthermore, plotting the normalized currents of MCU and mRyR1 as a function of Ca^{2+} concentration revealed that the open probability of mRyR1 peaks in the presence of 10–30 μM Ca^{2+}, whereas the MCU is fully activated at much higher concentrations of Ca^{2+} (above 100 μM Ca^{2+}).[22] These data suggest that the MCU with its low affinity and high capacity for mitochondrial Ca^{2+} uptake is better suited for reducing a possible cytosolic Ca^{2+} overload to prevent necrotic or apoptotic cell death.[43]

Last, the question arose which IP_3R subtype was involved. In accordance with the literature, we were able to demonstrate via real-time PCR, that all three IP_3R subtypes were expressed in murine ventricular myocytes. The Molkentin laboratory,[23] which generated the IP_3-sponge transgenic animals, described a general down-regulation of the IP_3Rs without differentiating between the different subtypes. In this study, we demonstrated that IP_3R type 2 expression (the most abundant type in cardiac myocytes[1]) was decreased whereas IP_3R type 1 and 3 expression levels in IP_3-sponge mice were significantly increased compared with myocytes from WT mice. These data are in line with the findings of Drawnel *et al.*[44] who also found decreased IP_3R type 2 expression in these animals. As in the transgenic mouse model used by us, the produced IP_3-molecules are bound within the cytosol and cannot bind to their receptor, this up-regulation can represent a compensatory mechanism underlining the importance of IP_3R type 1 and 3 mediated signalling for the cell. Although, increased expression of IP_3Rs has been shown under pathological conditions, particularly in heart failure,[45] valvular heart disease,[46] and atrial fibrillation.[47] Our study provides the evidence, however, that under normal physiological conditions, IP_3R-mediated Ca^{2+} transfer to mitochondria leads to increased ATP generation in cardiac myocytes.

Altogether, our data indicate that constitutive activity of IP_3Rs is important for modulation of cellular energetics in cardiac myocytes. Furthermore, our result that IP_3R–mRyR1 crosstalk is responsible for the maintenance of ATP levels in cardiac myocytes could actually explain the recent puzzling discoveries why MCU knockout mice do not reveal any significant bioenergetical problems in their hearts.[48] To conclude, we were able to demonstrate a new signalling pathway through which mitochondria of cardiac myocytes can decode Ca^{2+} signals of the cell and thus are able to adapt their function to the whole cell's energetic needs.

4.1 Study limitations

Ca^{2+} indicators used in this study are non-ratiometric fluorescent dyes, and therefore were not calibrated. With non-ratiometric dyes, we could not account for the possible dye leakage from the cells and bleaching, thus it is not appropriate to convert the fluorescent signal into Ca^{2+} concentration in terms of millimolar. Therefore, changes in Ca^{2+} are reported as background corrected fluorescence levels normalized to basal levels.

Supplementary material

Supplementary material is available at *Cardiovascular Research* online.

Conflict of interest: none declared.

Funding

This project was funded by the Interdisciplinary Center for Clinical Research (IZKF) Würzburg (project number Z3-19), the Comprehensive Heart Failure Centre (CHFC), the American Heart Association Grant-in-Aid 15GRNT25090220 (to E.N.D), and the Rudolph Virchow Center for Experimental Biomedicine.

References

1. Kockskämper J, Zima AV, Roderick HL, Pieske B, Blatter LA, Bootman MD. Emerging roles of inositol 1,4,5-trisphosphate signaling in cardiac myocytes. *J Mol Cell Cardiol* 2008;**45**:128–147.
2. Kockskämper J, Seidlmayer L, Walther S, Hellenkamp K, Maier LS, Pieske B. Endothelin-1 enhances nuclear Ca2+ transients in atrial myocytes through Ins(1,4,5)P3-dependent Ca2+ release from perinuclear Ca2+ stores. *J Cell Sci* 2008;**121**:186–195.
3. Wu X, Zhang T, Bossuyt J, Li X, McKinsey TA, Dedman JR, Olson EN, Chen J, Brown JH, Bers DM. Local InsP3-dependent perinuclear Ca2+ signaling in cardiac myocyte excitation-transcription coupling. *J Clin Invest* 2006;**116**:675–682.
4. Harzheim D, Talasila A, Movassagh M, Foo RS-Y, Figg N, Bootman MD, Roderick HL. Elevated InsP3R expression underlies enhanced calcium fluxes and spontaneous extra-systolic calcium release events in hypertrophic cardiac myocytes. *Channels Austin Tex* 2010;**4**:67–71.
5. Gilbert JC, Shirayama T, Pappano AJ. Inositol trisphosphate promotes Na-Ca exchange current by releasing calcium from sarcoplasmic reticulum in cardiac myocytes. *Circ Res* 1991;**69**:1632–1639.
6. Proven A, Roderick HL, Conway SJ, Berridge MJ, Horton JK, Capper SJ, Bootman MD. Inositol 1,4,5-trisphosphate supports the arrhythmogenic action of endothelin-1 on ventricular cardiac myocytes. *J Cell Sci* 2006;**119**:3363–3375.
7. Denton RM, McCormack JG. Ca^{2+} as a second messenger within mitochondria of the heart and other tissues. *Annu Rev Physiol* 1990;**52**:451–466.
8. Kirichok Y, Krapivinsky G, Clapham DE. The mitochondrial calcium uniporter is a highly selective ion channel. *Nature* 2004;**427**:360–364.
9. Gunter TE, Sheu S-S. Characteristics and possible functions of mitochondrial Ca^{2+} transport mechanisms. *Biochim Biophys Acta BBA—Bioenerg* 2009;**1787**:1291–1308.
10. Ryu S-Y, Beutner G, Kinnally KW, Dirksen RT, Sheu S-S. Single channel characterization of the mitochondrial ryanodine receptor in heart mitoplasts. *J Biol Chem* 2011;**286**:21324–21329.
11. Jean-Quartier C, Bondarenko AI, Alam MR, Trenker M, Waldeck-Weiermair M, Malli R, Graier WF. Studying mitochondrial Ca(2+) uptake—a revisit. *Mol Cell Endocrinol* 2012;**353**:114–127.
12. Dedkova EN, Blatter LA. Mitochondrial Ca^{2+} and the heart. *Cell Calcium* 2008;**44**:77–91.
13. Dash RK, Qi F, Beard DA. A biophysically based mathematical model for the kinetics of mitochondrial calcium uniporter. *Biophys J* 2009;**96**:1318–1332.
14. Pradhan RK, Qi F, Beard DA, Dash RK. Characterization of Mg2+ inhibition of mitochondrial Ca2+ uptake by a mechanistic model of mitochondrial Ca^{2+} uniporter. *Biophys J* 2011;**101**:2071–2081.
15. Pradhan RK, Qi F, Beard DA, Dash RK. Characterization of membrane potential dependency of mitochondrial Ca^{2+} uptake by an improved biophysical model of mitochondrial Ca^{2+} uniporter. *PLoS One* 2010;**5**:e13278.
16. Csordás G, Várnai P, Golenár T, Sheu S-S, Hajnóczky G. Calcium transport across the inner mitochondrial membrane: molecular mechanisms and pharmacology. *Mol Cell Endocrinol* 2012;**353**:109–113.
17. Favaron M, Bernardi P. Tissue-specific modulation of the mitochondrial calcium uniporter by magnesium ions. *FEBS Lett* 1985;**183**:260–264.
18. Boelens AD, Pradhan RK, Blomeyer CA, Camara AKS, Dash RK, Stowe DF. Extramatrix Mg^{2+} limits Ca^{2+} uptake and modulates Ca^{2+} uptake-independent respiration and redox state in cardiac isolated mitochondria. *J Bioenerg Biomembr* 2013;**45**:203–218.
19. Luongo TS, Lambert JP, Yuan A, Zhang X, Gross P, Song J, Shanmughapriya S, Gao E, Jain M, Houser SR, Koch WJ, Cheung JY, Madesh M, Elrod JW. The mitochondrial calcium uniporter matches energetic supply with cardiac workload during stress and modulates permeability transition. *Cell Rep* 2015;**12**:23–34.
20. Kwong JQ, Lu X, Correll RN, Schwanekamp JA, Vagnozzi RJ, Sargent MA, York AJ, Zhang J, Bers DM, Molkentin JD. The mitochondrial calcium uniporter selectively matches metabolic output to acute contractile stress in the heart. *Cell Rep* 2015;**12**:15–22.
21. Tewari SG, Camara AKS, Stowe DF, Dash RK. Computational analysis of Ca^{2+} dynamics in isolated cardiac mitochondria predicts two distinct modes of Ca^{2+} uptake. *J Physiol* 2014;**592**:1917–1930.
22. Beutner G, Sharma VK, Lin L, Ryu S-Y, Dirksen RT, Sheu S-S. Type 1 ryanodine receptor in cardiac mitochondria: transducer of excitation-metabolism coupling. *Biochim Biophys Acta* 2005;**1717**:1–10.
23. Nakayama H, Bodi I, Maillet M, DeSantiago J, Domeier TL, Mikoshiba K, Lorenz JN, Blatter LA, Bers DM, Molkentin JD. The IP3 receptor regulates cardiac hypertrophy in response to select stimuli/novelty and significance. *Circ Res* 2010;**107**:659–666.
24. Zhou Z, Matlib MA, Bers DM. Cytosolic and mitochondrial Ca^{2+} signals in patch clamped mammalian ventricular myocytes. *J Physiol* 1998;**507**(pt. 2):379–403.

25. Csordás G, Renken C, Várnai P, Walter L, Weaver D, Buttle KF, Balla T, Mannella CA, Hajnóczky G. Structural and functional features and significance of the physical linkage between ER and mitochondria. *J Cell Biol* 2006;**174**:915–921.
26. Rizzuto R, Pinton P, Carrington W, Fay FS, Fogarty KE, Lifshitz LM, Tuft RA, Pozzan T. Close contacts with the endoplasmic reticulum as determinants of mitochondrial Ca^{2+} responses. *Science* 1998;**280**:1763–1766.
27. McCormack JG, Denton RM. The effects of calcium ions and adenine nucleotides on the activity of pig heart 2-oxoglutarate dehydrogenase complex. *Biochem J* 1979;**180**:533–544.
28. Seidlmayer L, Blatter LA, Pavlov E, Dedkova E. Inorganic polyphosphate-an unusual suspect of the mitochondrial permeability transition mystery. *Channels Austin Tex* 2012;**6**:463–467.
29. Azzolin L, von Stockum S, Basso E, Petronilli V, Forte MA, Bernardi P. The mitochondrial permeability transition from yeast to mammals. *FEBS Lett* 2010;**584**:2504–2509.
30. Zima AV, Pabbidi MR, Lipsius SL, Blatter LA. Effects of mitochondrial uncoupling on Ca(2+) signaling during excitation-contraction coupling in atrial myocytes. *Am J Physiol Heart Circ Physiol* 2013;**304**:H983–H993.
31. Dedkova EN, Blatter LA. Measuring mitochondrial function in intact cardiac myocytes. *J Mol Cell Cardiol* 2012;**52**:48–61.
32. Balaban RS. The role of Ca(2+) signaling in the coordination of mitochondrial ATP production with cardiac work. *Biochim Biophys Acta* 2009;**1787**:1334–1341.
33. Ryu S-Y, Beutner G, Dirksen RT, Kinnally KW, Sheu S-S. Mitochondrial ryanodine receptors and other mitochondrial Ca^{2+} permeable channels. *FEBS Lett* 2010;**584**:1948–1955.
34. Seidlmayer LK, Juettner V, Kettlewell S, Pavlov E, Blatter LA, Dedkova EN. Distinct mPTP activation mechanisms in ischemia-reperfusion: contributions of Ca^{2+}, ROS, pH and inorganic polyphosphate. *CVR* 2015;**106**:237–248.
35. O-Uchi J, Jhun BS, Hurst S, Bisetto S, Gross P, Chen M, Kettlewell S, Park J, Oyamada H, Smith GL, Murayama T, Sheu S-S. Overexpression of ryanodine receptor type 1 enhances mitochondrial fragmentation and Ca2+-induced ATP production in cardiac H9c2 myoblasts. *Am J Physiol Heart Circ Physiol* 2013;**305**:H1736–H1751.
36. Santulli G, Xie W, Reiken SR, Marks AR. Mitochondrial calcium overload is a key determinant in heart failure. *Proc Natl Acad Sci U S A* 2015;**112**: 11389–11394.
37. Domeier TL, Roberts CJ, Gibson AK, Hanft LM, McDonald KS, Segal SS. Dantrolene suppresses spontaneous Ca^{2+} release without altering excitation-contraction coupling in cardiomyocytes of aged mice. *Am J Physiol Heart Circ Physiol* 2014;**307**: H818–H829.
38. Sedova M, Dedkova EN, Blatter LA. Integration of rapid cytosolic Ca^{2+} signals by mitochondria in cat ventricular myocytes. *Am J Physiol Cell Physiol* 2006;**291**:C840–C850.
39. Szalai G, Krishnamurthy R, Hajnóczky G. Apoptosis driven by IP(3)-linked mitochondrial calcium signals. *EMBO J* 1999;**18**:6349–6361.
40. Hajnóczky G, Hager R, Thomas AP. Mitochondria suppress local feedback activation of inositol 1,4, 5-trisphosphate receptors by Ca^{2+}. *J Biol Chem* 1999;**274**:14157–14162.
41. Fill M, Copello JA. Ryanodine receptor calcium release channels. *Physiol Rev* 2002;**82**:893–922.
42. Lanner JT, Georgiou DK, Joshi AD, Hamilton SL. Ryanodine receptors: structure, expression, molecular details, and function in calcium release. *Cold Spring Harb Perspect Biol* 2010;**2**:a003996.
43. Gunter TE, Gunter KK, Sheu SS, Gavin CE. Mitochondrial calcium transport: physiological and pathological relevance. *Am J Physiol* 1994;**267**:C313–C339.
44. Drawnel FM, Wachten D, Molkentin JD, Maillet M, Aronsen JM, Swift F, Sjaastad I, Liu N, Catalucci D, Mikoshiba K, Hisatsune C, Okkenhaug H, Andrews SR, Bootman MD, Roderick HL. Mutual antagonism between IP(3)RII and miRNA-133a regulates calcium signals and cardiac hypertrophy. *J Cell Biol* 2012;**199**:783–798.
45. Go LO, Moschella MC, Watras J, Handa KK, Fyfe BS, Marks AR. Differential regulation of two types of intracellular calcium release channels during end-stage heart failure. *J Clin Invest* 1995;**95**:888–894.
46. Lamirault G, Gaborit N, Le Meur N, Chevalier C, Lande G, Demolombe S, Escande D, Nattel S, Léger JJ, Steenman M. Gene expression profile associated with chronic atrial fibrillation and underlying valvular heart disease in man. *J Mol Cell Cardiol* 2006;**40**:173–184.
47. Yamda J, Ohkusa T, Nao T, Ueyama T, Yano M, Kobayashi S, Hamano K, Esato K, Matsuzaki M. Up-regulation of inositol 1,4,5 trisphosphate receptor expression in atrial tissue in patients with chronic atrial fibrillation. *J Am Coll Cardiol* 2001;**37**:1111–1119.
48. Pan X, Liu J, Nguyen T, Liu C, Sun J, Teng Y, Fergusson MM, Rovira II, Allen M, Springer DA, Aponte AM, Gucek M, Balaban RS, Murphy E, Finkel T. The physiological role of mitochondrial calcium revealed by mice lacking the mitochondrial calcium uniporter. *Nat Cell Biol* 2013;**15**:1464–1472.